

Spectral and structural studies of nickel(II) complexes of salicylaldehyde 3-azacyclothiosemicarbazones

Leji Latheef, Maliyeckal R. Prathapachandra Kurup *

Department of Applied Chemistry, Cochin University of Science and Technology, Kochi 682 022, Kerala, India

Received 12 June 2007; accepted 17 August 2007

Available online 24 October 2007

Abstract

Mononuclear nickel(II) complexes with two ONS donor thiosemicarbazone ligands {salicylaldehyde 3-hexamethyleneiminyl thiosemicarbazone [H₂L¹] and salicylaldehyde 3-tetramethyleneiminyl thiosemicarbazone [H₂L²]} have been prepared and physico-chemically characterized. IR and electronic spectra of the complexes have been obtained. The thiosemicarbazones bind to the metal as dianionic ONS donor ligands in all the complexes except in [Ni(HL¹)₂] (**1**). In compound **1**, the ligand is coordinated as a mono-anionic (HL⁻) one. The magnetic susceptibility measurements indicate that all the complexes are mononuclear and are diamagnetic. The complexes were given the formulae [Ni(HL¹)₂] (**1**), [NiL¹py] (**2**), [NiL¹α-pic] (**3**), [NiL¹γ-pic]·H₂O (**4**), [NiL²py] (**5**) and [NiL²γ-pic] (**6**). The structures of compounds **2** and **3** have been solved by single crystal X-ray crystallography and were found to be distorted square planar in geometry with coordination of azomethine nitrogen, thiolato sulfur, phenolato oxygen and pyridyl nitrogen atoms.

© 2007 Elsevier Ltd. All rights reserved.

Keywords: Thiosemicarbazone; Nickel(II) complex; Salicylaldehyde; Crystal structure

1. Introduction

The coordination chemistry of thiosemicarbazones with transition metals [1–4], which began with Jensen's work [5], has been more intensively investigated as compared to that of main group elements [6,7]. Thiosemicarbazones are an important group of multidentate ligands with potential binding sites available for a wide variety of metal ions [8–10]. These thiourea derivatives find substantial applications in different facets of contemporary scientific research. Thiosemicarbazones and their metal complexes are a broad class of biologically active compounds [4]. Due to this biological activity, there is considerable interest in metal complexes of heterocyclic thiosemicarbazones [4]. Nickel(II) complexes containing sulfur donors have received considerable attention due

to the identification of a sulfur rich coordination environment in biological nickel centres, such as the active sites of certain ureases, methyl-S-coenzyme-M-methyl reductase and hydrogenases [11].

Spectral and, in some complexes, structural investigations of a series of nickel(II) complexes of ONS donor thiosemicarbazones [12–16] have been reported earlier. The thiosemicarbazone ligand usually coordinates with the metal through the imine nitrogen and sulfur atom. The ligands feature more than two covalent sites, the number of which depends on the aldehyde and on the tautomeric equilibrium of the thiosemicarbazone, although the most common way to coordinate is through the thiolate form [17]. We have reported Cu(II) [18] and Zn(II) [19] complexes of the present thiosemicarbazone ligands recently. Here, we report six mononuclear nickel (II) complexes of salicylaldehyde 3-hexamethyleneiminyl and 3-tetramethyleneiminyl thiosemicarbazones. These complexes were characterized by IR, electronic and magnetic data.

* Corresponding author. Tel.: +91 484 2575804; fax: +91 484 2577595.
E-mail address: mrp@cusat.ac.in (M.R. Prathapachandra Kurup).

2. Experimental

2.1. Materials

All the solvents used for the synthesis of the thiosemicarbazone ligands and their complexes were purified by distillation. Pyridine, $\alpha/\beta/\gamma$ -picoline, $\text{Ni}(\text{OAc})_2 \cdot 4\text{H}_2\text{O}$ (Central drug house) were used as received. 4-Methyl-4-phenyl-3-thiosemicarbazide was prepared as reported previously [20].

2.2. Synthesis of the ligands

H_2L^1 was prepared using a reported procedure [21]. H_2L^2 was prepared as described by adapting the reported procedure [20,21]. A solution of 4-methyl-4-phenyl thiosemicarbazide (1 g, 5.52 mmol) in acetonitrile (5 ml) was treated with salicylaldehyde (0.60 ml, 5.52 mmol) and pyrrolidine (0.50 ml, 5.52 mmol) and refluxed for 20 min. The solution was allowed to cool and the fine colorless needles of the compound separated out. It was filtered off, washed with cold acetonitrile and dried *in vacuo* over P_4O_{10} . The compound was recrystallized from methanol. The structures of the two ligands are given in Scheme 1.

2.3. Synthesis of complexes

Complex **1** was prepared by refluxing an ethanolic solution of H_2L^1 with a methanolic solution of $\text{Ni}(\text{OAc})_2 \cdot 4\text{H}_2\text{O}$ in a 2:1 molar ratio for 4 h. The brown colored complex that formed was filtered, washed with ethanol and then with ether and dried over P_4O_{10} *in vacuo*. The complexes **2–6** were prepared by refluxing an ethanolic solution of the corresponding ligands and heterocyclic bases with a methanolic solution of $\text{Ni}(\text{OAc})_2 \cdot 4\text{H}_2\text{O}$ in a 1:1:1 molar ratio. The complexes that separated were filtered, washed with ethanol and finally with ether and dried over P_4O_{10} *in vacuo*. Crystals suitable for X-ray analysis for compounds **2** and **3** were obtained by slow evaporation of solutions of the compounds from an ethanol methanol mixture (1:1 v/v) over 10 days.

The colors and analytical data of the complexes, elemental analysis and magnetic susceptibilities are presented in Table 1.

2.4. Physical measurements

Elemental analyses were carried out using a Vario EL III CHN analyzer at SAIF, Kochi, India. Magnetic suscep-

Table 1
Stoichiometries, colors and partial elemental analysis of complexes

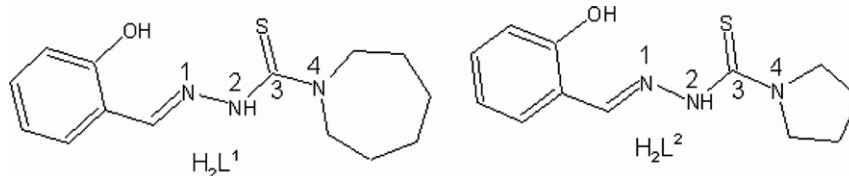
Compound	Anal. Found (Calc.) (%)		
	C	H	N
$[\text{Ni}(\text{HL}^1)_2]$ (1)	55.9(55.30)	6.36(5.93)	14.04(13.74)
$[\text{NiL}^1\text{py}]$ (2)	55.20(55.23)	5.35(5.37)	13.55(13.56)
$[\text{NiL}^1\alpha\text{-pic}]$ (3)	56.21(56.23)	5.63(5.66)	13.11(13.12)
$[\text{NiL}^1\gamma\text{-pic}] \cdot \text{H}_2\text{O}$ (4)	54.11(53.90)	6.02(5.89)	12.59(12.58)
$[\text{NiL}^2\text{py}]$ (5)	53.12(53.02)	4.57(4.71)	14.42(14.55)
$[\text{NiL}^2\gamma\text{-pic}]$ (6)	54.02(54.16)	5.70(5.05)	14.16(14.04)

tibility measurements were carried out at IIT, Roorkee, India, at 298 K in the polycrystalline state on a PAR model 155 Vibrating sample magnetometer at 5 kOe field strength using $\text{Hg}[\text{Co}(\text{SCN})_4]$ as a calibrant. The FT-IR spectra were recorded on a Thermo Nicolet AVATAR 370 DTGS FTIR spectrometer using KBr pellets in the range 400–4000 cm^{-1} at SAIF, Cochin University of Science and Technology, Kochi 22, India, and far IR spectra were recorded in the range 50–500 cm^{-1} on a Nicolet Magna 550 FT-IR spectrophotometer using polyethylene pellets at SAIF, IIT, Bombay, India. Electronic spectra were recorded on a UVD-3500 UV-VIS-Double beam Spectrophotometer from solutions in DMF. ^1H NMR spectra were recorded on a Bruker AMX 300 in CDCl_3 with TMS as an internal standard.

2.5. X-ray crystallography

Reddish brown crystals of compounds **2** and **3**, having approximate dimensions of $0.26 \times 0.21 \times 0.17$ and $0.35 \times 0.30 \times 0.20 \text{ mm}^3$, respectively, were selected. The crystal data for compounds **2** and **3** were collected by Crysalis CCD, Oxford Diffraction Ltd. with graphite-monochromated $\text{Mo K}\alpha$ ($\lambda = 0.71073 \text{ \AA}$) radiation. In compound **2**, the atom C10 in the ring containing N3 is disordered as this carbon splits over two sets of positions. Restraints were applied to assist the geometry of the disordered atom. The ratio of major to minor disorder components for the C10 atom is 54:46. Compound **3** similarly has some disorder in the 7-membered ring. Even though refinement with restraints was applied to the 7-membered ring, the problems of the weak data could not be improved further. In spite of several attempts, we were unable to isolate single crystals of good quality.

In both of these compounds restraints were applied to assist the geometry of the disordered atoms. The trial structure was solved using SHELXS-97 [22] and refinement was



Scheme 1. The thiosemicarbazones H_2L^1 and H_2L^2 .

Table 2
Crystal data for compounds **2** and **3**

	(2)	(3)
Empirical formula	C ₁₉ H ₂₂ N ₄ NiOS	C ₂₀ H ₂₄ N ₄ NiOS
Formula weight	826.35	427.20
Temperature (K)	150(2)	150(2)
Wavelength (Å)	0.71073	0.71073
Crystal system	orthorhombic	monoclinic
Space group	<i>Pbca</i>	<i>P2₁/a</i>
<i>Unit cell dimensions</i>		
<i>a</i> (Å)	13.7965(19)	10.567(3)
<i>b</i> (Å)	21.954(4)	10.933(3)
<i>c</i> (Å)	25.410(5)	17.439(6)
α (°)	90	90
β (°)	90	100.42(3)
γ (°)	90	90
Volume (Å ³)	7696(2)	1981.5(10)
<i>Z</i>	16	4
<i>D</i> _{calc} (g/cm ³)	1.426	1.432
Absorption coefficient (mm ⁻¹)	1.132	1.102
<i>F</i> (000)	3456	896
Crystal size (mm ³)	0.26 × 0.21 × 0.17	0.35 × 0.30 × 0.20
θ Range for data collection (°)	2.95–25	3.02–2
Index ranges	–16 ≤ <i>h</i> ≤ 16, –26 ≤ <i>k</i> ≤ 25, –30 ≤ <i>l</i> ≤ 19	–12 ≤ <i>h</i> ≤ 12, –13 ≤ <i>k</i> ≤ 12, –20 ≤ <i>l</i> ≤ 20
Reflections collected	37350	17298
Independent reflections (<i>R</i> _{int})	6769 (0.0865)	3476 (0.1093)
Refinement method	full-matrix on <i>F</i> ²	full-matrix on <i>F</i> ²
Data/restraints/parameters	6769/0/479	3476/52/232
Goodness-of-fit on <i>F</i> ²	0.761	0.787
Final <i>R</i> indices [<i>I</i> > 2σ(<i>I</i>)]	<i>R</i> ₁ = 0.0362, <i>wR</i> ₂ = 0.0636	<i>R</i> ₁ = 0.0600, <i>wR</i> ₂ = 0.1418
<i>R</i> indices (all data)	<i>R</i> ₁ = 0.1028, <i>wR</i> ₂ = 0.0732	<i>R</i> ₁ = 0.1798, <i>wR</i> ₂ = 0.1691

carried out by full-matrix least squares on *F*² (SHELXL) [22]. The molecular and crystal structures are illustrated by DIAMOND version 3.1d [23] and MERCURY [24]. All non-hydrogen atoms were refined anisotropically and hydrogen atoms were geometrically fixed at calculated positions. The crystallographic data and structure refinement parameters for the complexes are given in Table 2.

3. Results and discussion

The elemental analyses data are consistent with the general empirical formula [M(HL)₂] for **1**, MLB for **2**, **3**, **4**, **5** and **6** where M is the nickel metal atom, L is the doubly deprotonated thiosemicarbazone ligand and B is the heterocyclic bases *viz.* py and $\alpha/\beta/\gamma$ pic. All the nickel complexes are reddish brown in color, which is common for complexes involving thiosemicarbazone coordination, resulting from the sulfur to metal charge transfer bands [25]. The complexes are insoluble in most common solvents. They are however soluble in DMF and DMSO.

The room temperature magnetic moments of the Ni(II) complexes suggest that they are all essentially diamagnetic. For the d⁸ electronic configuration, diamagnetism generally implies that the metal ion has a square-planar configuration. The electronic spectra of the complexes in DMF solution are not well resolved owing to very intense charge transfer bands extending into the visible portion of the spectra.

3.1. Crystal structure of the compound [NiL¹py] and [NiL¹ α -pic]

The molecular structures of [NiL¹py] (**2**) and [NiL¹ α -pic] (**3**) along with the atom labelling schemes are shown in Figs. 1 and 2, and selected bond lengths and bond angles are summarized in Table 3. The ligand H₂L¹ gets doubly deprotonated to behave as an ONS tridentate ligand, coordinating *via* its phenolato oxygen, azomethine nitrogen and thiolate sulfur atom in the deprotonated form after thiol formation, giving a distorted square planar geometry around the nickel atom. The fourth coordination site is occupied by the nitrogen atom from the heterocyclic bases. The *E* configuration of the thiosemicarbazone chain about the C7–N1 bond is retained to facilitate the coordination of the thiolate sulfur to Ni in the two complexes. This reveals that no rotation has occurred about the azomethine bond for coordination. The coordination results in one 5-membered and one 6-membered chelate ring in the two complexes.

Compound **2** crystallizes with two monomers per asymmetric unit in the orthorhombic crystal system. The two molecules in the asymmetric unit are almost identical. So the discussion can be limited to one of the molecules. The Ni1 coordination is almost square planar with a maximum mean deviation of the coordinating atoms (phenolic oxygen O1, azomethine nitrogen N1, thiolate sulfur S1 and

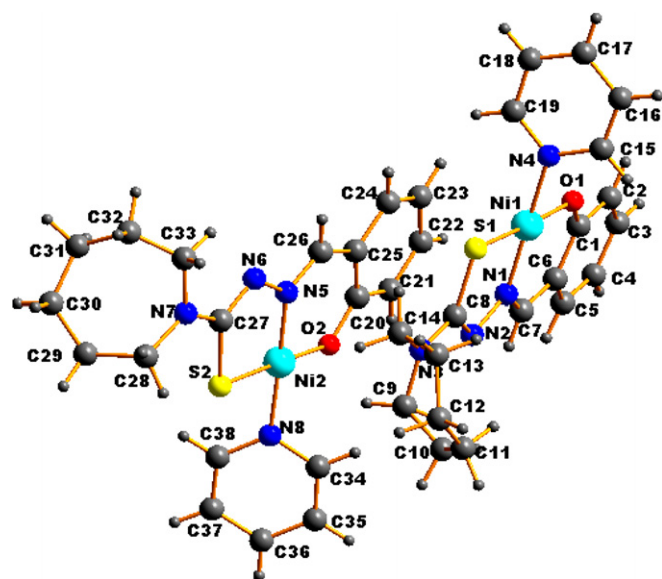


Fig. 1. Molecular structure of compound **2**.

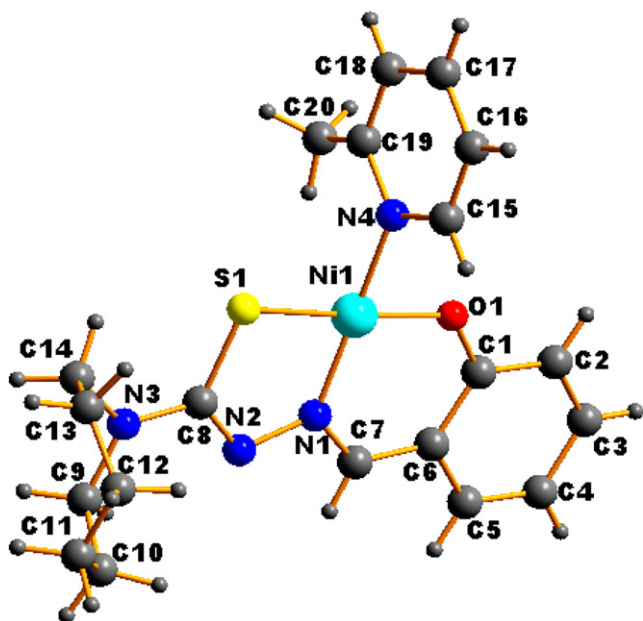


Fig. 2. Molecular structure of compound 3.

pyridyl nitrogen N4) from their own plane of 0.0103 Å for N4. The thiosemicarbazone moiety, C7–N1–N2–C8–S1–N3, also is almost planar and has a maximum mean plane deviation of 0.037(4) Å and an angle of 2.86(6)° to the plane of the four donor atoms, while the phenyl ring has an angle of 6.29(10)° to the donor plane of compound 2 indicating that the thiosemicarbazone moieties are close to coplanar with the nickel's coordination plane. Ring puckering analysis and least-square plane calculations show that the Cg(5) ring comprising of atoms N3, C9, C10, C11, C12, C13 and C14, and the Cg(10) ring comprising of atoms N7, C28, C29, C30, C31, C32 and C33 adopt a chair conformation [$Q_T = 0.696(6)$ Å (Cg(5)) and $Q_T = 0.650(6)$ Å (Cg(10))].

The bond angles O1–Ni1–N1 [96.16(12)°], O1–Ni1–N4 [85.35(11)°] and N1–Ni1–S1 [87.08(10)°] also reveal the distortion of the square plane comprising of Ni1, O1, S1, N1 and N4. The dihedral angle formed by the least square planes Cg(1) comprising of atoms Ni1, S1, N1, N2 and C8, and Cg(2) comprising of atoms Ni1, O1, N1, C1, C6 and C7 is 3.47(12)°. The C7–N1 bond distance of 1.305(4) Å lengthens compared to the corresponding C7–N1 bond distance (1.269(3) Å) in the ligand. The delocalization of electron density from the coordinating nitrogen onto the central metal atom gives rise to an elongated N1–N2 bond length (1.406(3) Å) compared to the uncomplexed thiosemicarbazone (1.356(3) Å). Also, the C7–N1–N2 bond angle decreases considerably compared to the ligand H_2L^1 . The loss of the proton bound to N2 in H_2L^1 produces a negative charge which is delocalized on the N1–N2–C8 system. This is indicated by the lengthening of the bond C8–S1, 1.753(4) Å, compared to the value of 1.684(3) Å in the ligand. This thiolate formation is also supported by the decrease in bond length of N2–C8, 1.304(4) Å from the value of 1.362(3) Å found in the

Table 3
Comparison of selected bond lengths (Å) and bond angles (°) for H_2L^1 , 2 and 3

	H_2L^1 ^a	2	3
<i>Bond lengths</i>			
Ni1–O1		1.837(2)	1.859(4)
Ni1–N1		1.848(3)	1.847(5)
Ni1–N4		1.907(3)	1.906(4)
Ni1–S1		2.134(11)	2.151(2)
Ni2–O2		1.848(2)	
Ni2–N5		1.859(3)	
Ni2–N8		1.925(3)	
Ni2–S2		2.132(11)	
S1–C8	1.684(3)	1.753(4)	1.759(6)
S2–C27		1.752(4)	
N1–C7	1.269(3)	1.305(4)	1.320(7)
N1–N2	1.356(3)	1.406(3)	1.393(6)
N2–C8	1.362(3)	1.304(4)	1.302(7)
N3–C8		1.350(4)	1.362(7)
N4–C19		1.326(4)	1.388
N4–C15		1.327(4)	1.392
N5–C26		1.302(4)	
N5–N6		1.400(4)	
N6–C27		1.293(4)	
N7–C27		1.357(4)	
N8–C34		1.340(4)	
N8–C38		1.343(4)	
<i>Bond angles</i>			
O1–Ni1–N1		96.56(12)	96.5(2)
O1–Ni1–N4		85.35(11)	87.56(19)
N1–Ni1–N4		177.87(12)	174.4(2)
O1–Ni1–S1		176.35(8)	176.71(14)
N1–Ni1–S1		87.08(10)	86.77(19)
N4–Ni1–S1		91.01(8)	89.17(15)
O2–Ni2–N5		95.75(12)	
O2–Ni2–N8		86.96(11)	
N5–Ni2–N8		177.26(14)	
O2–Ni2–S2		176.83(8)	
N5–Ni2–S2		87.15(11)	
N8–Ni2–S2		90.16(9)	
C8–S1–Ni1		96.57(13)	95.8(3)
C27–S2–Ni2		96.11(16)	
C7–N1–N2	120.0(2)	113.3(3)	112.4(5)
N2–N1–Ni1		122.8(2)	123.8(4)
C26–N5–N6		113.6(3)	
C26–N5–Ni2		124.0(3)	
N6–N5–Ni2		122.4(2)	
C26–N5–N6		113.6(3)	

^a Ref. [17].

uncomplexed thiosemicarbazone. The bond angles O1–Ni1–N4 [85.35(11)°] and S1–Ni1–N1 [87.08(10)°] are also analogous, as expected on the basis of the similar square planar nature for all the complexes. Coordination of O1 results in O1–C1 decreasing by approximately 0.04–0.05 Å.

Compound 3 crystallizes with only one monomer per asymmetric unit in the monoclinic crystal system. The bond angles N1–Ni1–O1 [96.5(2)°], O1–Ni1–N4 [87.56(19)°] and N1–Ni1–S1 [86.77(19)°] reveal the distortion of the square planar geometry. The dihedral angle formed by the least square planes Cg(1) comprising of atoms Ni1, S1, N1, N2 and C8, and Cg(2) comprising of atoms Ni1, O1, N1, C1, C6 and C7 is 0.6(2)°. Similar to compound 2, the

C7–N1 bond length increases compared to the ligand. Thus on complexation, the azomethine C–N bond lengthens because of coordination of the azomethine nitrogen. Coordination lengthens the thiosemicarbazone moiety's C8–S1 bond length to 1.759(6) Å and shortens the N2–C8 bond length to 1.302(7) Å. The maximum deviation from the least square planes around the Ni(II) ion is 0.0626(5) Å for N1. The thiosemicarbazonato moiety, C7–N1–N2–C8–S1–N3, is almost planar with a maximum mean deviation of 0.028(6) for N2 and is at an angle of 1.46(9)° to the plane of the four donor atoms, while the dihedral angle formed by the phenyl ring is 1.95(2)° to the donor plane. The hexamethyleneiminyl ring adopts a chair conformation [$Q_T = 0.7269$ Å].

The dihedral angles formed by the least square planes Cg(1) and Cg(2) for the compounds support the distorted square planar conformation for these complexes, where greater distortion is observed for compound **2**. This small deviation from coplanarity would certainly not hinder the delocalization of electrons in the coordination sphere, and the stability of the complex is sustained.

The Ni–N_{azomethine} bond lengths are shorter compared to the Ni–N_{base} bond lengths, indicating greater strength of the former bonds compared to the latter in the two complexes. The O1–Ni1–N1 bond angles are slightly greater compared to the similar Ni(II) ONS donor complexes [Ni(PTSC)(PPh₃)] 95.32(9)°, [Ni(PTSC)(PPh₃)]·CHCl₃, 95.4(1)° [12] and [Ni(C₁₈H₁₈N₆O₂S₂)](ClO₄)₂·2CH₄O, 83.64(12)° [26], and the N1–Ni1–S1 bond angles are comparable. The N1–Ni1–S1 bond angles are greater compared to [Ni(Et-fbt)₂], 85.35(11)°, [Ni(fbt)₂], 84.90(10)° [27] and [Ni(NQTS)₂]·2DMSO 81.47(16)° [28]. The C–N_{azomethine}

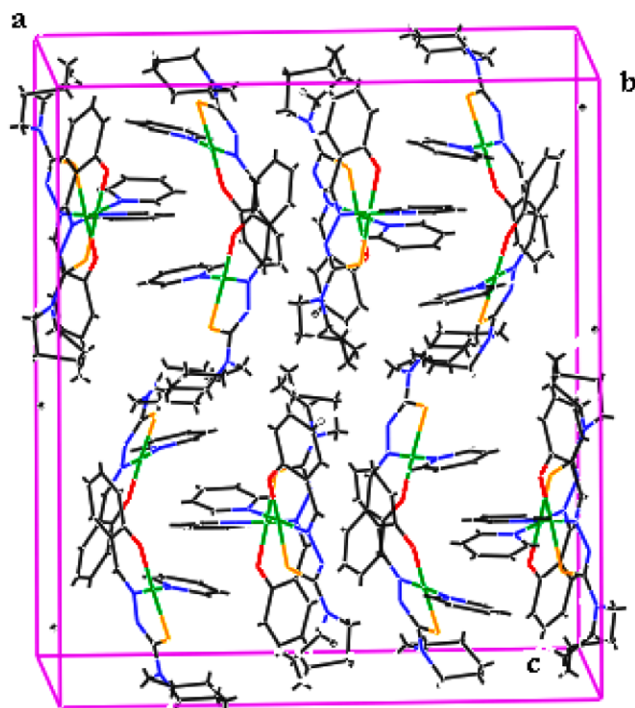


Fig. 3. Unit cell packing diagram of compound **2**.

bond length is shorter compared to other C–N_{py} bond lengths in the complexes. This indicates that the bonding is dominated by the thiosemicarbazone moiety.

In compound **2**, adjacent molecules are arranged in an offset manner within the unit cell when viewed along the *a* axis, as seen in Fig. 3, as a result of diverse π – π stacking, CH– π and hydrogen bonding interactions (Table 4).

The molecules of **3** are connected by various hydrogen bonding interactions and are arranged parallel along the *a* axis (Fig. 4). Though π – π interactions exist in the lattice of compound **3**, they are observed at distances greater than 4.0 Å, also there are no effective CH– π interactions (Table 5). adjacent molecules are arranged opposing directions within the unit cell.

3.2. Infrared spectra

The characteristic IR bands (50–4000 cm^{−1}) for the four free ligands differ from those of their complexes and pro-

Table 4
Interaction parameters of compound **2**

Cg(I)–Res 1...Cg (J)	Cg–Cg (Å)	α (°)	β (°)
π – π interactions			
Cg(1) [1] → Cg(9) ^a	3.747(2)	3.28	25.77
Cg(2) [1] → Cg(9) ^a	3.624(2)	6.74	24.05
Cg(3) [1] → Cg(8) ^b	3.856(2)	17.19	27.64
Cg(8) [1] → Cg(3) ^b	3.856(2)	17.19	12.31
Cg(9) [1] → Cg(1) ^c	3.747(2)	3.28	22.53
Cg(9) [1] → Cg(2) ^c	3.624(2)	6.74	24.30

Equivalent position code: $a = 1/2 - x, 1/2 + y, z$; $b = 1/2 + x, y, 1/2 - z$; $c = 1/2 - x, -1/2 + y, z$

α = Dihedral angle between planes I and J (°)

β = \angle Cg(I) → Cg(J) or Cg(I) → Me vector and normal to plane I (°)

Cg(1) = Ni1, S1, C8, N2, N1; Cg(2) = Ni1, O1, C1, C6, C7, N1;

Cg(3) = N4, C15, C16, C17, C18, C19

Cg(8) = N8, C34, C35, C36, C37, C38; Cg(9) = C20, C21, C22, C23, C24, C25

XH(I)...Cg(J)	H...Cg (Å)	X–H...Cg (°)	X...Cg (Å)
CH – π interactions			
C(17)–H(17) [1] → Cg(6) ^a	2.69	144	3.4857
C(18)–H(18) [1] → Cg(1) ^a	2.69	139	3.4420
C(35)–H(35) [1] → Cg(9) ^a	2.67	153	3.5223
C(37)–H(37) [1] → Cg(4) ^a	2.90	141	3.6669

Equivalent position code: $a = 1/2 + x, y, 1/2 - z$

Cg(1) = Ni1, S1, C8, N2, N1; Cg(4) = C1, C2, C3, C4, C5, C6;

Cg(6) = Ni2, S2, C27, N6, N5; Cg(9) = C20, C21, C22, C23, C24, C25

D–H...A	D...H (Å)	H...A (Å)	D...A (Å)	D–H...A (°)
H -bonding				
C15–H15...O2 ^a	0.930	2.967(2)	3.539(5)	121.23(25)
C16–H16...O2 ^a	0.930	2.827(2)	3.460(5)	126.33(26)
C3–H3...N7 ^b	0.930	2.895(3)	3.589(5)	132.41(26)
C17–H17...N5 ^c	0.930	2.755(3)	3.530(6)	141.42(29)
C18–H18...N1 ^c	0.930	2.962(3)	3.445(5)	113.90(27)
C18–H18...N2 ^c	0.930	2.859(3)	3.424(5)	120.36(28)
C36–H36...O1 ^c	0.930	2.863(2)	3.723(5)	154.33(25)
C19–H19...N2 ^c	0.930	2.699(3)	3.358(5)	128.52(24)

D, donor; A, acceptor. Equivalent position code: $a = x, y, z$; $b = x, 1/2 - y, 1/2 + z$; $c = 1/2 + x, -z + 1/2 + 1$.

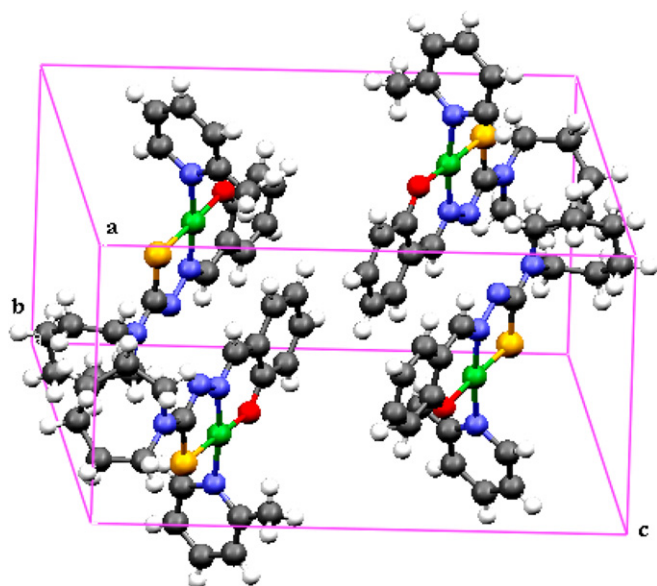


Fig. 4. Unit cell packing diagram of compound 3.

Table 5
Interaction parameters of the compound 3

D–H···A	D···H (Å)	H···A (Å)	D···A (Å)	D–H···A (°)
<i>H-bonding</i>				
C14–H14B···S1 ^a	0.970	2.517(2)	3.021(8)	112.25(47)
C14–H14A···N2 ^b	0.970	2.867(6)	3.540(11)	127.27(48)
C(17)–H17···N2 ^c	0.930	2.858(5)	3.771(7)	167.25(27)
C18–H18···O1 ^d	0.930	2.732(5)	3.596(9)	154.94(47)

D, donor, A, acceptor, Equivalent position code: a = x, y, z; b = x – 1/2, –y + 1/2, +z; c = x, y – 1, z; d = x – 1/2, –y – 1/2, +z.

vide significant indications regarding the bonding sites of the ligands. IR spectral assignments of the ligands and the complexes are listed in Table 6. A medium band in the range 3070–3160 cm⁻¹ in the free ligands, due to the ν(²NH) vibration, disappears in the spectra of the complexes, providing strong evidence for ligand coordination around the Ni(II) ion in its deprotonated form.

The IR spectra of the ligands H₂L¹ and H₂L² exhibit intermolecular hydrogen bonded ν(OH) vibrations at 3315 and 3232 cm⁻¹, respectively, which disappear in the spectra of the complexes except for **1**. It is further corrob-

Table 6
IR spectroscopic assignments for the ligands and their nickel complexes

Compound	ν(C=N _{azo})	ν(C=N)	ν(N–N)	ν/δ[(C=S)/(C–S)]	ν(C–O)	ν(Ni–N)	ν(Ni–O)	ν(Ni–S)	Bands due to heterocyclic base
H ₂ L ¹	1612		1037	1324, 861	1271				
[Ni(HL ¹) ₂] (1)	1581	1530	1071	1267, 753	1270	466		350	
[NiL ¹ py] (2)	1597	1536	1070	1288, 757	1207	463	430	345	1447, 691
[NiL ¹ α-pic] (3)	1601	1531	1063	1278, 752	1209	494	446	347	1448, 614
[NiL ¹ γ-pic]·H ₂ O (4)	1597	1537	1068	1270, 753	1208	460	420	332	1449, 714
H ₂ L ²	1622		1034	1338, 839	1288				
[NiL ⁴ py] (5)	1600	1538	1061	1290, 758	1210	490	422	334	1478, 693
[NiL ⁴ γ-pic] (6)	1600	1538	1055	1275, 757	1205	476	425	325	1480, 607

orated with the decrease in stretching frequency by 60–80 cm⁻¹ for ν(CO) as well as the appearance of a band in the 410–430 cm⁻¹ region due to a ν(Ni–O) stretch in the spectra of the complexes [29]. It indicates coordination *via* the phenolic oxygen. In complex **1**, the phenolic group is not coordinated to the metal. The non-involvement of the phenolic group of the same thiosemicarbazone ligand in a zinc complex [19] has been proven by us. However, there is X-ray crystal structure evidence for the existence of the phenol rather than the phenolate form in a closely related salicylaldehyde thiosemicarbazone [30], with the ligand acting as an ONS donor.

On coordination of the azomethine nitrogen, ν(C=N_{azo}) shifts to lower wavenumbers by 10–20 cm⁻¹, as the band shifts from 1613 cm⁻¹ in the uncomplexed thiosemicarbazone spectrum to ~1596 cm⁻¹ in the spectra of the complexes. Coordination of the azomethine nitrogen is confirmed by the presence of a new band in the range 450–490 cm⁻¹, assignable to ν(Ni–N) for these complexes [31]. The ν(N–N) band of the thiosemicarbazone is found in the 1030–1075 cm⁻¹ range. The increase in the frequency of this band in the spectra of the complexes, due to the increase in the bond strength, again confirms coordination *via* the azomethine nitrogen [19].

The bands in the ranges 1320–1340 and 835–865 cm⁻¹ due to thioamide {which is partly ν(C=S)} stretching and bending vibrations, respectively, of the free ligands are shifted to lower values, indicating coordination of the thiolate sulfur to the Ni(II) ion. This negative shift of ν(CS) in the complexes has already been indicated by Campbell [1]. Coordination *via* the thiolato sulfur is confirmed with the presence of a new band in the range 320–350 cm⁻¹, assignable to ν(Ni–S) for these complexes [32]. In all the Ni(II) complexes, another strong band is found in the range 1530–1540 cm⁻¹, which may be due to the newly formed ν(C=N) bond formed as a result of enolization. The IR spectra of the complexes, except **1**, display bands characteristic of coordinated heterocyclic bases [33].

3.3. Electronic spectra

The electronic spectral assignments of the ligands and their complexes are given in Table 7. The thiosemicarbazones show a ring π → π* band at ~36000 cm⁻¹ and an

Table 7
Electronic spectral assignments of the ligands and their Ni(II) complexes

Compound	$\pi-\pi^*$	$n-\pi^*$	LMCT	d-d
H_2L^1	36110	29500		
$[Ni(HL^1)_2]$ (1)	35340	30210	26190	17240
$[NiL^1py]$ (2)	34840	30400	26450	16980
$[NiL^1\alpha-pic]$ (3)	35420	30920, 33000	23640, 26700	17060
$[NiL^1\gamma-pic] \cdot H_2O$ (4)	35580	30960, 33330	23980, 26740	17070
H_2L^2	36490	30210		
$[NiL^2py]$ (5)	36020	32680	23790, 26040	18480
$[NiL^2\gamma-pic]$ (6)	36230	30210, 33780	23980, 26380	18520

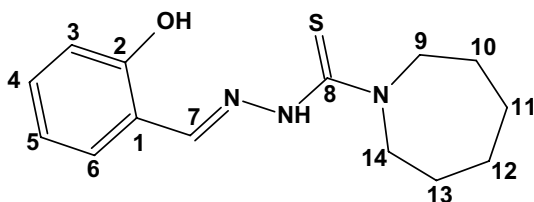


Fig. 5. The structure of the ligand H_2L^1 along with atom labelling scheme.

$n \rightarrow \pi^*$ band (involving transitions within the thiosemicarbazone moiety, mainly C(7)=N(1) and C(8)–S groups [16]) at $\sim 30000\text{ cm}^{-1}$. These bands are slightly shifted upon complexation. The shift of the $\pi \rightarrow \pi^*$ bands to a longer wavelength region in the complexes is the result of the C–S bond being weakened and the conjugation system being enhanced on complexation [34,35]. The $n \rightarrow \pi^*$ bands in the complexes show a blue shift due to donation of the lone pair of electrons to the metal and hence the coordination of the azomethine with a reduction of intensity.

In the case of complexes having ONS donor ligands, two ligand to metal charge transfer bands are found in

the 25000–28000 and 23000–24500 cm^{-1} ranges. Their positions are dependent on the steric requirements of the N(4) substituents. That is, thiosemicarbazones with bulkier N(4)-substituents have these bands at somewhat higher energies. In most of the dianionic complexes, LMCT maxima of the phenolate complexes show line broadening with a tail running into the visible part of the spectrum. This may result from a phenolate to Ni(II) LMCT band being superimposed on the low energy side of the $S \rightarrow Ni(II)$ LMCT. Each complex has a broad d–d combination band that appears as a shoulder on the intraligand and charge-transfer bands. These nickel complexes show a trend of increasing size of the N(4)-substituent and lower energy of the d–d band maximum, presumably due to weakening of the coordinate bonding with increased bulkiness of the ligands. The absence of bands below 10000 cm^{-1} confirms the square planar nature of the complexes [36,37].

3.4. 1H NMR spectra

The numbering scheme used in the 1H NMR spectrum of the ligand H_2L^1 is given in Fig. 5 and the spectra of the complexes 1 and 4 are given in Figs. 6 and 7. The 1H NMR spectrum of the ligand H_2L^1 has been discussed earlier [19]. 1H NMR spectral assignments of the ligand and its Ni(II) complexes 1 and 4 are given in Table 8. The signals for 2NH are absent from the spectra of these complexes, as expected, and the phenolic OH is absent in the spectrum of complex 4 because of its loss on complex formation, which is an evidence for the coordination of the ligand as a doubly deprotonated anion. The spectra of complexes 1 and 4 show a sharp singlet which integrates as one hydrogen at δ 7.44 and 7.83 ppm,

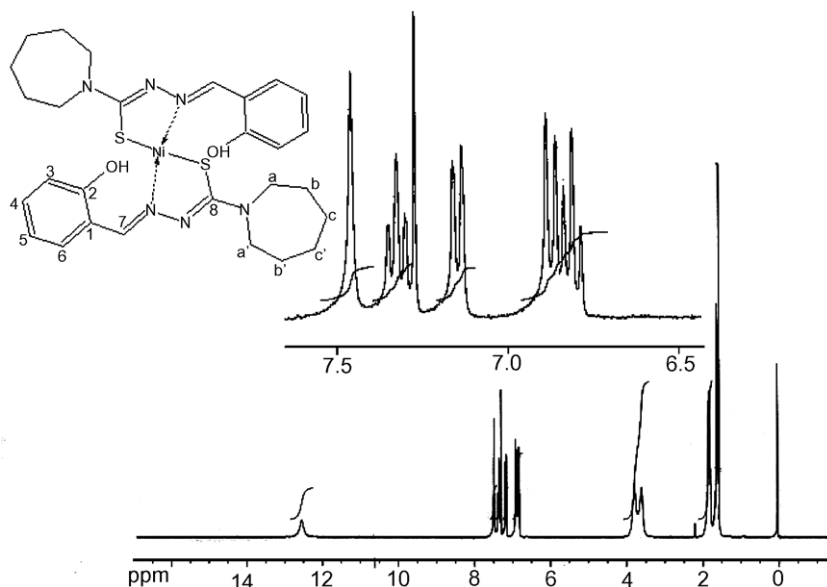


Fig. 6. 1H NMR spectrum of compound 1.

Table 8
 ^1H NMR (CDCl_3) assignments of the ligand H_2L^1 and its Ni(II) complexes (δ in ppm)

Compound	OH	Aromatic protons				$^8\text{CH}=\text{}$	$^a\text{CH}_2$	$^b\text{CH}_2$	$^c\text{CH}_2$
		H^6Ph	H^4Ph	H^3Ph	H^5Ph				
H_2L^1	11.3	7.09	6.97	6.80	6.67	7.99	3.63	1.66	1.42
$[\text{Ni}(\text{HL}^1)_2]$ (1)	12.51	7.45	7.31	7.13	6.82	7.45	3.67	1.79	1.56
$[\text{NiL}^1\gamma\text{-pic}] \cdot \text{H}_2\text{O}$ (4)		7.25	7.18	7.14	6.80	7.83	3.61	1.74	1.55

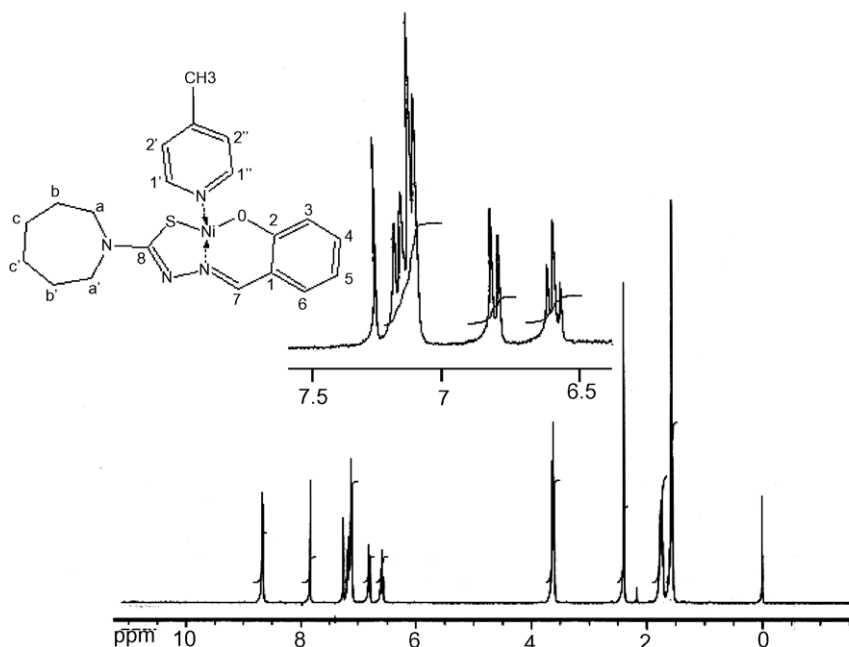


Fig. 7. ^1H NMR spectrum of compound **4**.

respectively, corresponding to $^7\text{CH}=\text{}$ present in the thiosemicarbazone moiety. Complex **1** shows a peak at δ 12.51 ppm due to the presence of the uncoordinated hydroxyl group. The more downfield shift of the OH protons compared to the uncomplexed thiosemicarbazone may be due to the overall loss of electron density and hydrogen bonding interactions. The ^1H NMR spectrum of **1** shows a multiplet which integrates as two hydrogens at δ ca. 6.82 ppm and is assigned to the protons attached to ^3C and ^5C of the phenyl ring. ^4CH and ^6CH protons of the phenyl ring appear at δ 7.13 and 7.31 ppm, respectively. In complex **4**, the protons of the aromatic ring ^3CH and ^5CH appear at δ 6.58 and 6.80 ppm. The spectrum also shows a multiplet which integrates as four hydrogens at δ ca. 7.15 ppm, corresponding to ^4CH , ^6CH and the base protons $\text{H}^{2'}$ and $\text{H}^{2''}$. The upfield shift of these base protons may be due to the presence of the electron releasing methyl group present in the pyridine ring. The heterocyclic base protons ($\text{H}^{1'}$ and $\text{H}^{1''}$) are present as a doublet, which integrates as two hydrogens at δ 8.66 ppm. The downfield shift of these protons may be the result of the withdrawal of electron density from the thiosemicarbazone moiety and the heterocyclic base, due to coordination with the metal atom [38]. Methyl protons appear as a singlet at δ 2.38 ppm (see Fig. 7).

Acknowledgements

L. Latheef thanks the Council of Scientific and Industrial Research, New Delhi, India, for financial support in the form of a fellowship. M.R.P. Kurup is thankful to the CSIR, New Delhi, India, for financial support. The authors also thank the National Single Crystal X-ray diffraction Facility, IIT, Bombay, for X-ray data collection.

Appendix A. Supplementary material

CCDC 603882 and 604196 contain the supplementary crystallographic data for **2** and **3**. The data can be obtained free of charge at www.ccdc.cam.ac.uk/conts/retrieving.html, or from the Cambridge Crystallographic Data Centre (CCDC), 12 Union Road, Cambridge, CB2, IEZ, UK fax: (+44)-1223-336-033; e-mail: deposit@ccdc.cam.ac.uk. Supplementary data associated with this article can be found, in the online version, at [doi:10.1016/j.poly.2007.08.048](https://doi.org/10.1016/j.poly.2007.08.048).

References

- [1] M.J.M. Campbell, *Coord. Chem. Rev.* 15 (1975) 279.
- [2] S. Padhye, G.B. Kauffman, *Coord. Chem. Rev.* 63 (1985) 127.

- [3] D.X. West, S.B. Padhye, P.B. Sonawane, *Struct. Bond.* (Berlin) 76 (1991) 4.
- [4] D.X. West, A.E. Liberta, S.B. Padhye, R.C. Chikate, P.B. Sonawane, A.S. Kumbhar, R.G. Yerande, *Coord. Chem. Rev.* 123 (1993) 49.
- [5] K.A. Jensen, E. Rancke-Madsen, *Z. Anorg. Allerg. Chem.* 219 (1934) 243.
- [6] C.E. Holloway, M. Melnik, *J. Organomet. Chem.* 495 (1995) 1.
- [7] C.E. Holloway, M. Melnik, *Main Group Met. Chem.* 17 (1994) 799.
- [8] J.S. Casas, M.S. Garcia-Tasende, J. Sordo, *Coord. Chem. Rev.* 209 (2000) 197.
- [9] A. Sreekanth, S. Sivakumar, M.R.P. Kurup, *J. Mol. Struct.* 655 (2003) 47.
- [10] R.P. John, A. Sreekanth, M.R.P. Kurup, A. Usman, I.A. Razak, H.K. Fun, *Spectrochim. Acta* 59A (2003) 1349.
- [11] A.D. Naik, S.M. Annigeri, U.B. Gangadharmath, V.K. Revankar, V.B. Mahale, *J. Mol. Struct.* 616 (2002) 119.
- [12] R. Prabhakaran, R. Karvenmbu, T. Hashimoto, K. Shimizu, K. Natarajan, *Inorg. Chim. Acta* 358 (2005) 2093.
- [13] E. Labisbal, K.D. Haslow, A. Sousa-Pedrares, J. Valdes- Martinez, A.H. Ortega, D.X. West, *Polyhedron* 22 (2003) 2831.
- [14] D.X. West, Y. Yang, T.L. Klein, K.I. Goldberg, A.E. Liberta, J. Valdes-Martinez, S.H. Ortega, *Polyhedron* 14 (1995) 3051.
- [15] D.E. Barber, Z. Lu, T. Richardson, R.H. Crabtree, *Inorg. Chem.* 31 (1992) 4709.
- [16] P. Bindu, M.R.P. Kurup, *Indian J. Chem.* 36A (1997) 1094.
- [17] A.G. Quiroga, C.N. Ranninger, *Coord. Chem. Rev.* 248 (2004) 119.
- [18] L. Latheef et al., *Spectrochim. Acta* (2007), doi:10.1016/j.saa.2007.07.015.
- [19] L. Latheef et al., *Polyhedron* (2007), doi:10.1016/j.poly.2007.05.023.
- [20] J.P. Scovill, *Phosphorus Sulfur Silicon Relat. Elem.* 60 (1991) 15.
- [21] L. Latheef, E. Manoj, M.R.P. Kurup, *Acta Crystallogr. C* 62 (2006) 16.
- [22] G.M. Sheldrick, *SHELXL-97 and SHELXS-97 Program for the Solution of Crystal Structures*, University of Göttingen, Germany, 1997.
- [23] K. Brandenburg, *DIAMOND version 3.1d*, Crystal Impact GbR, Bonn, Germany, 2006.
- [24] C.F. Macrac, P.R. Edgington, P. McCabe, E. Pidcock, G.P. Shields, R. Taylor, M. Towler, J. Van de Streek, *J. Appl. Cryst.* 39 (2006) 453.
- [25] V. Suni, M.R.P. Kurup, M. Nethaji, *Polyhedron* 26 (2007) 3097.
- [26] X.-H. Qiu, H.-Y. Wu, *Acta Crystallogr. E* 60 (2004) m 1151.
- [27] M.B. Ferrari, S. Capacchi, F. Bisceglie, G. Pelosi, P. Tarasconi, *Inorg. Chim. Acta* 312 (2001) 81.
- [28] Z. Afrasiabi, E. Sinn, W. Lin, Y. Ma, C. Campana, S. Padhye, *J. Inorg. Biochem.* 99 (2005) 1526.
- [29] M. Mikuriya, H. Okawa, S. Kida, *Bull. Chem. Soc. Jpn.* 53 (1980) 3717.
- [30] M. Zimmer, G. Schulte, X.-L. Luo, R.H. Crabtree, *Angew. Chem., Int. Ed. Engl.* 30 (1991) 193.
- [31] P. Sousa, J.A. Garcia-Vasquez, J.R. Masaguer, *Trans. Met. Chem.* 9 (1984) 318.
- [32] R. Roy, M. Chaudhury, S.K. Mondal, K. Nag, *J. Chem. Soc., Dalton Trans.* (1984) 1681.
- [33] P.B. Sreeja, M.R.P. Kurup, *Spectrochim. Acta* 61A (2005) 331.
- [34] V. Philip, V. Suni, M.R.P. Kurup, *Polyhedron* 25 (2006) 1931.
- [35] I.-X. Li, H.A. Tang, Yi-Zhi Li, M. Wang, L.-F. Wang, C.-G. Xia, *J. Inorg. Biochem.* 78 (2000) 167.
- [36] B.S. Garg, M.R.P. Kurup, S.K. Jain, Y.K. Bhoon, *Trans. Met. Chem.* 16 (1991) 111.
- [37] H.B. Gray, C.J. Bauhausen, *J. Am. Chem. Soc.* 85 (1963) 260.
- [38] D.X. West, Y. Yang, T.L. Klein, K.I. Goldberg, A.E. Liberta, J. Valdes-Martinez, R.A. Toscano, *Polyhedron* 14 (1995) 1681.